Effects of adjacent bubble on spatiotemporal evolutions of mechanical stresses surrounding bubbles oscillating in tissues

Qing-Qin Zou(邹青钦), Shuang Lei(雷双), Zhang-Yong Li(李章勇), and Dui Qin(秦对)[†]

Department of Biomedical Engineering, School of Bioinformatics, Chongqing University of Posts and Telecommunications, Chongqing 400065, *China*

(Received 31 March 2022; revised manuscript received 25 April 2022; accepted manuscript online 18 May 2022)

The cavitation dynamics and mechanical stress in viscoelastic tissues, as the primary mechanisms of some ultrasound therapies, are extremely complex due to the interactions of cavitation bubble with adjacent bubbles and surrounding tissues. Therefore, the cavitation dynamics and resultant mechanical stress of two-interacting bubbles in the viscoelastic tissues are numerically investigated, especially focusing on the effects of the adjacent bubble. The results demonstrate that the mechanical stress is highly dependent on the bubble dynamics. The compressive stress and tensile stress are generated at the stage of bubble expansion and collapse stage, respectively. Furthermore, within the initial parameters examined in this paper, the effects of the adjacent bubble will distinctly suppress the radial expansion of the small bubble and consequently lead its associated stresses to decrease. Owing to the superimposition of two stress fields, the mechanical stresses surrounding the small bubble in the direction of the neighboring bubble are smaller than those in other directions. For two interacting cavitation bubbles, the suppression effects of the nearby bubble on both the cavitation dynamics and the stresses surrounding the small bubble increase as the ultrasound amplitude and the initial radius of the large bubble increase, whereas they decrease with the inter-bubble distance increasing. Moreover, increasing the tissue viscoelasticity will reduce the suppression effects of the nearby bubble, except in instances where the compressive stress and tensile stress first increase and then decrease with the tissue elasticity and viscosity increasing respectively. This study can provide a further understanding of the mechanisms of cavitation-associated mechanical damage to the adjacent tissues or cells.

Keywords: cavitation dynamics, cavitation-induced mechanical stress, effects of the nearby bubble, viscoelastic tissues

PACS: 43.35.+d, 47.55.dd, 87.50.Y– **DOI:** 10.1088/1674-1056/ac70ba

1. Introduction

Acoustic cavitation refers to the formation of bubbles/cavities and subsequent bubble dynamics involving growth, oscillation and collapse in a medium, subjected to ultrasound waves with amplitudes exceeding a certain threshold value.[1,2] It has been extensively studied in some scientific areas and increasingly utilized in various areas, such as ultrasonic cleaning,[3] food processing,[4] ultrasound imaging and therapy,[5–7] as well as cavitation-assisted chemical reactions, dialysis, and extraction.[8] In biomedicine, acoustic cavitation and its biophysical effects are the main mechanisms responsible for the therapeutic applications of ultrasound, such as localized drug delivery,[9] gene transfection,[10] opening of the blood–brain barrier,[11] sonothrombolysis,[12] lithotripsy,[13] and histotripsy.[14] Specifically, a series of secondary motions can result from the acoustic cavitation (*e.g.*, microstreaming, shock waves, and liquid microjets), concomitantly producing mechanical effects on surrounding tissues or cells, which are paramount to therapeutic outcomes.[9–14] At relatively low acoustic pressures, the bubble oscillates around its equilibrium radius with small oscillation amplitudes (*i.e.* stable cavitation), giving rise to microstreaming in the surrounding medium.[9–11] This motion in turn imposes shear stresses on the adjacent structures and probably causes reversible damages, consequently enabling to facilitate the transport of therapeutic agents across some biologically inaccessible barriers, *e.g.*, cell membrane, blood–brain barrier.[9–11] When the acoustic pressure amplitude exceeds a certain threshold, the inertial cavitation occurs in which bubble expands rapidly and collapses violently.[12–14] During inertial cavitation, microjet and shockwaves can be generated, which might cause irreversible and serious damages to the adjacent cells or tissues for ultrasound therapies with the objective of generating extreme mechanical changes in the target region (*e.g.*, sonothrombolysis, lithotripsy, histotripsy).[12–14] Thus, appropriate utilization of the acoustic cavitation and its mechanical effects is crucial in achieving different biomedical applications, in which different damage mechanisms are involved and the cavitation-associated mechanical effects may need maximizing, controlling, or preventing entirely.

Experimental observations have indicated that local deformations in the vicinity of cavitation bubbles are considerable and can damage the adjacent cells or tissues subjected to the high stress, strain, and strain rate.[15–17] However, it is extremely difficult to experimentally investigate the cavitation dynamics and its associated mechanical effects *in vivo* due to the micro-scale bubbles oscillating on a microsecond time scale, the opacity of tissues, and the lack of appropriate techniques to measure the stress, strain and strain rate.[18–20]

[†]Corresponding author. E-mail: duiqin@cqupt.edu.cn

© 2023 Chinese Physical Society and IOP Publishing Ltd

To better understand the mechanisms of tissue damage, numerical simulation has been performed to investigate the single bubble dynamics and quantify the spatiotemporal evolutions of the stress, strain, and strain rate fields in the surrounding tissues *via* coupling the Keller–Miksis equation with the Kelvin–Voigt viscoelastic model.[18–20] These studies demonstrated that the cavitation-associated mechanical effects (*i.e.*, stress, strain, and strain rate) are highly dependent on the tissue viscoelasticity and bubble dynamics.[18–20] Note that the Kelvin–Voigt model can only describe the creep behavior of the viscoelastic tissues. Considering that the stress relaxation of tissue can also influence the dynamic behaviors of cavitation bubbles,[21–23] in this study the Zener model is adopted to simulate the viscoelastic tissue due to its superiority in describing both the creep behavior and stress relaxation of the viscoelastic tissue.[21–23]

In the aforementioned applications of acoustic cavitation, the multiple bubbles or even a bubble cloud are generally generated.[5,7,9–13,16] Thus, the effects of adjacent bubbles (*i.e.*, the bubble–bubble interactions) on the bubble dynamics should also be taken into account. The bubble–bubble interaction means that each bubble emits pressure wave to surrounding medium which acts on the neighboring bubbles as an additional pressure.[24–32] Thus, by introducing the pressures emitted by each bubble at the location of the other bubble, the cavitation model of two-interacting bubbles in a viscoelastic tissue has been well-established for investigating the radial pulsations and/or translational motions of bubbles.[22,33–35] The results demonstrated that both the bubble–bubble interactions and the tissue viscoelasticity will suppress the radial bubble oscillations.[22,34] Furthermore, the suppression effect of the bubble–bubble interaction could be dramatically reduced with the tissue elasticity and/or viscosity increasing.[22,34] Additionally, the studies also demonstrated that the translational motions of bubbles are negligible *in vivo*, due to the high viscoelasticity of the tissues.[22,34] Therefore, the attention is mainly focused on the radial pulsations of bubbles in the present study as described in previous study.[33] More importantly, in addition to the cavitation dynamics of the two-interacting bubbles, the spatiotemporal evolutions of the resultant mechanical stresses in the viscoelastic tissues are also crucial in understanding the mechanisms of cavitation-induced mechanical damages to the adjacent cells or tissues.

The spatial distributions of the cavitation-associated stresses will be extremely complex not only due to the bubble–bubble interaction affecting bubble dynamics, but also due to the superposition effects of the stress fields generated by multiple cavitation bubbles. In this study, the cavitation dynamics of two-interacting bubbles is investigated *via* a comprehensive model simultaneously considering both the tissue viscoelasticity and the bubble–bubble interaction. Subsequently, the spatiotemporal evolution of the mechanical stress generated by two-interacting bubbles in the surrounding tissue is characterized quantitatively by superimposing two stress fields surrounding each bubble. Furthermore, two variables (*i.e.*, the absolute variation of bubble expansion ratio and the absolute variation of maximum stress magnitude) are introduced to characterize the effects of the adjacent bubble on the cavitation dynamics and the resultant stress in the surrounding tissue. Additionally, the influences of the ultrasound amplitude, inter-bubble distance, initial radius of the large bubble and tissue viscoelasticity are also examined.

2. Theory and methods

2.1. Cavitation model of two-interacting bubbles in viscoelastic tissues

Figure 1 shows the schematic of two-interacting cavitation bubbles and the associated mechanical stresses in viscoelastic tissues. They are initially in equilibrium with initial radii (*i.e.* R_{i0} and R_{j0}) and an inter-bubble distance (*i.e.*, d_0). Under external ultrasonic excitation, both bubbles will exhibit radial oscillations over time (*i.e.*, $R_i(t)$ and $R_j(t)$) and interact with each other, resulting in mechanical stresses (*i.e.*, τ_i and τ_j) in the surrounding tissue. As described in previous studies,[22,34] it is assumed that the sphericities of both bubbles remain unchanged during their oscillations. Moreover, the evaporation/condensation and gas diffusion at the gas–liquid interfaces, chemical reactions inside the bubbles as well as the translational motions of bubbles are also assumed to be negligible in our work, similar to that in previous studies.[33] The Keller–Miksis equations coupled with the bubble–bubble interactions are used to describe the dynamics of two-interacting bubbles and given below:[34]

$$\begin{aligned}&\left(1-\frac{\dot{R}_i}{c}\right)R_i\ddot{R}_i+\left(\frac{3}{2}-\frac{\dot{R}_i}{2c}\right)\dot{R}_i^2-\frac{p_i}{\rho}\left(1+\frac{\dot{R}_i}{c}\right)-\frac{R_i\dot{p}_i}{\rho c}\\&=-\sum_{j=1,j\neq i}^{2}\frac{\left(R_j^2\ddot{R}_j+2R_j\dot{R}_j^2\right)}{d_0},\\&\text{for}\quad i=1,2\ \text{ and }\ j=3-i,\end{aligned}\tag{1}$$

where R_i and R_j denote the radius of the i-th bubble and j-th bubble, respectively. The dot denotes time derivative, c is the speed of the sound in medium, ρ is the density of medium, p_i is the pressure in the medium at the wall of the i-th bubble, and d_0 is the inter-bubble distance. Note that the time delays while the pressure radiated by one bubble propagating to the other bubble is neglected in Eq. (1), which are reasonable due to the small inter-bubble distances ($d_0 < 100$ μm) in this study, in which case the effect of time delay becomes insignificant.[34,36]

According to the mechanical equilibrium at the gas–liquid interface, the pressure at the wall of the i-th bubble p_i

can be described as[34]

$$p_i = p_{g,i} - \frac{2\sigma}{R_i} + \tau_{rr}|_{R_i} - p_0 - p_{ac}(t). \tag{2}$$

It is assumed that the gas inside both bubbles obeys the van der Waals equation, hence the gas pressure inside the i-th bubble $p_{g,i}$ is determined by[25,29,34,37]

$$p_{g,i} = \left(p_0 + \frac{2\sigma}{R_{i0}}\right)\left[\frac{(R_{i0}^3 - h_i^3)}{(R_i^3 - h_i^3)}\right]^{\kappa}, \tag{3}$$

where p_0 is the atmospheric pressure, R_{i0} is the initial radius of the i-th bubble, σ is the surface tension, h_i is the van der Waals hard core radius, κ is the polytropic exponent of the gas inside the bubble, $\tau_{rr}|_{R_i}$ denotes the radial stress at the i-th bubble interface, which is introduced to couple the cavitation model with the viscoelastic model. The acoustic pressure $p_{ac}(t) = -p_A \sin(2\pi f t)$, where p_A and f are the ultrasound amplitude and frequency, respectively.

2.2. Viscoelastic model for surrounding tissues

Several constitutive equations have been developed to describe the relationship of the stress with the strain in a viscoelastic medium (*e.g.* Maxwell, Kelvin–Voigt, Kelvin–Voigt-based Neo–Hookean, Zener models, and so on).[21,22,34,38–41] In the present study, the Zener model is used in this work due to its unique superiority in accurately describing the creep behavior and relaxation time of the viscoelastic tissue simultaneously[22]

$$\tau_{rr} + \lambda_1 \dot{\tau}_{rr} = 2G\gamma_{rr} + 2\mu\dot{\gamma}_{rr}, \tag{4}$$

where τ_{rr} and γ_{rr} are the mechanical stress and strain in the radial direction, respectively, the dot denotes the derivative with respect to time, λ_1, G, and μ are the relaxation time, elasticity, and viscosity of the viscoelastic tissue, respectively. According to the continuity equation, the $\dot{\gamma}_{rr} = -2R^2\dot{R}/r^3$ and $\gamma_{rr} = -2(R^3 - R_0^3)/3r^3$ can be derived.[21,22] Then substituting them into Eq. (4), the stress produced by the i-th and j-th bubble oscillations $\tau_{rr,i}$ and $\tau_{rr,j}$ can be described as follows:

$$\tau_{rr,i} + \lambda_1 \dot{\tau}_{rr,i} = -\frac{4G(R_i^3 - R_{i0}^3)}{3r_i^3} - \frac{4\mu R_i^2 \dot{R}_i}{r_i^3}, \tag{5}$$

$$\tau_{rr,j} + \lambda_1 \dot{\tau}_{rr,j} = -\frac{4G(R_j^3 - R_{j0}^3)}{3r_j^3} - \frac{4\mu R_j^2 \dot{R}_j}{r_j^3}, \tag{6}$$

where r_i and r_j denote the distance from the considered position Q to the i-th and j-th bubble centers, respectively. Accordingly, the radial stresses at the interfaces of i-th and j-th bubbles (*i.e.*, $\tau_{rr}|_{R_i}$ and $\tau_{rr}|_{R_j}$) can be calculated by substituting $r_i = R_i$ and $r_j = R_j$ into Eqs. (5) and (6), respectively, and the resulting equations are given below:

$$\tau_{rr}|_{R_i} + \lambda_1 \dot{\tau}_{rr}|_{R_i} = -\frac{4G}{3}\left(1 - \frac{R_{i0}^3}{R_i^3}\right) - \frac{4\mu\dot{R}_i}{R_i}, \tag{7}$$

$$\tau_{rr}|_{R_j} + \lambda_1 \dot{\tau}_{rr}|_{R_j} = -\frac{4G}{3}\left(1 - \frac{R_{j0}^3}{R_j^3}\right) - \frac{4\mu\dot{R}_j}{R_j}. \tag{8}$$

2.3. Evaluations of cavitation-associated stresses surrounding two-interacting bubbles

To calculate the mechanical stress in viscoelastic tissue generated by the two-interacting cavitation bubbles, it is assumed that there is a point Q in tissue with the position of (x, y), as displayed in Fig. 1. The distances from the i-th and j-th bubble centers to the point Q described as r_i and r_j respectively can be split into two terms,

$$r_i = R_i(t) + r_{i,b}, \tag{9}$$

$$r_j = R_j(t) + r_{j,b}, \tag{10}$$

where $r_{i,b}$ and $r_{j,b}$ denote the distance from the considered position Q to the i-th and j-th bubble walls, respectively. Submitting these conditions into Eqs. (5) and (6), one can obtain the stresses in tissues produced by the i-th and j-th bubbles as denoted by τ_i and τ_j in Fig. 1. Note that the point Q will simultaneously experience the stresses generated by the acoustic cavitation of both two bubbles, so that the total stress can be described as

$$\tau = \tau_i + \tau_j. \tag{11}$$

Note that the indexes i and j are interchangeable and they denote the numbers of the bubbles (*i.e.* $\{1,2\}$ or $\{2,1\}$).

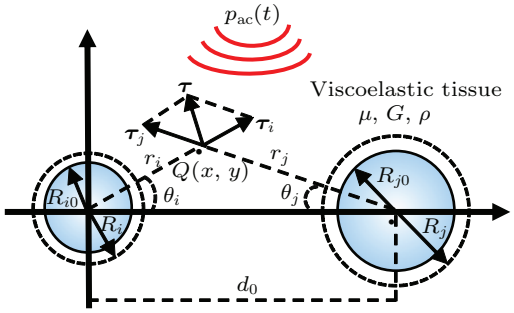


Fig. 1. Schematic diagram of two-interacting cavitation bubbles and associated mechanical stresses in viscoelastic tissues.

2.4. Methods of investigating bubble dynamics and cavitation-associated stress

The cavitation-associated stress is closely related to the bubble dynamics that can be evaluated by several important parameters,[42–45] such as the expansion ratio (R_{max}/R_0), relative expansion ratio ($R_{max} - R_0)/R_0$, compression ratio (R_{max}/R_{min}), and ratio of maximum oscillation radius to the collapse time (R_{max}^3/t_c). In the present study, the expansion ratio (R_{max}/R_0) represented by R' is chosen as a metric to characterize the cavitation dynamics. For the i-th bubble, it can be described as

$$R_i' = \frac{\max(R_i)}{R_{i0}}. \tag{12}$$

Similarly, the cavitation-associated stress in the surrounding tissue is characterized by the maximum of the stress magnitude, which is represented by τ' as indicated in previous researches.[18,19,46]

2.5. Simulation conditions

The numerical model for describing the cavitation dynamics of two-interacting bubbles and the cavitation-associated stresses in viscoelastic tissues are obtained by coupling Eqs. (1)–(3), (5)–(8), and (11). The model is numerically solved with the fourth-order Runge–Kutta method through using the ODE15s solver built in the commercial software MATLAB (The Math-Works, Natick, MA, USA) in time steps of $0.0001/f$, a relative tolerance of 10^{-12}, and an absolute tolerance of 10^{-12}. Unless otherwise specified, the physical parameters and their default values are set according to Table 1.[22,34]

Table 1. Parameters used in simulations.

Parameters	Values	Units	Parameters	Values	Units
f	1	MHz	c	1540	m/s
G	200	kPa	R_{10}	1	μm
p	1.013×10^5	Pa	R_{20}	5	μm
ρ	1060	kg/m^3	d_0	40	μm
σ	0.056	N/m	h_i	$R_{i0}/8.5$	μm
μ	15	mPa·s	p_A	1	MPa
λ_1	3	ns	κ	1.4	/

3. Results and discussion

3.1. Effects of bubble–bubble interactions on cavitation dynamics

The representative cavitation dynamics of two bubbles with different initial radii ($R_{10} = 1$ μm and $R_{20} = 5$ μm) for two cases with (w) and without (w/o) considering the bubble–bubble interactions, are presented in Fig. 2. It is evident that the maximum radius of the small bubble with the consideration of the bubble–bubble interactions ($R_{1,w}$) is significantly smaller than that of the other case ($R_{1,w/o}$) as shown in Fig. 2(a). Correspondingly, the wall velocity of the small bubble influenced by the adjacent bubble ($v_{1,w}$) is much smaller than the case where the bubble–bubble interaction is not taken into account ($v_{1,w/o}$) as displayed in Fig. 2(c). For the time-varying radius and wall velocity of the large bubble, figures 2(b) and 2(d) demonstrate that the differences between the cases with and without considering the bubble–bubble interaction are indistinguishable. The results indicate that the effects of the adjacent bubble with large initial radius will notably suppress the cavitation dynamics of the small bubble, which accord well with the previous studies.[29,34] Moreover, it may be reasonable to deduce that the cavitation-associated mechanical stress in the surrounding tissues will be prominently affected since it is highly dependent on the cavitation dynamics,[18,19,46] thus the effect of the adjacent bubble on the stress is examined in the following sections.

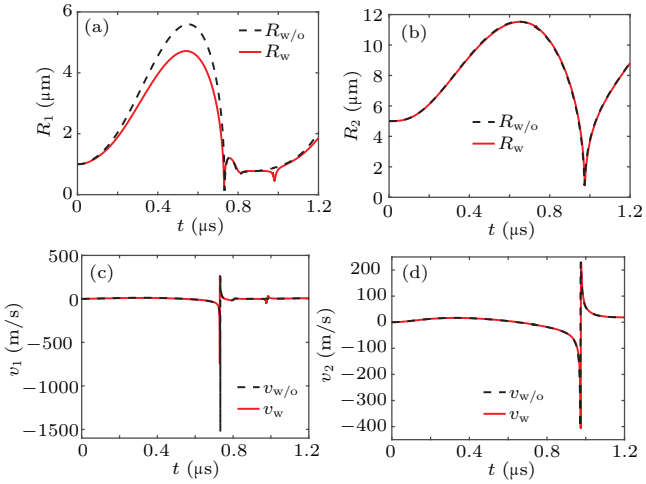


Fig. 2. Comparation of bubble dynamics for two cases with and without considering the bubble–bubble interactions, including radii of (a) small and (b) large bubbles, as well as the wall velocities of (c) small and (d) large bubbles.

3.2. Spatiotemporal evolutions of cavitation-associated stresses in surrounding tissues

During the acoustic cavitation, the spatiotemporal distributions of the mechanical stresses surrounding two-interacting bubbles and two isolated bubbles ($R_{10} = 1$ μm and $R_{20} = 5$ μm) are presented in Fig. 3. The time-varying stresses surrounding the small and large bubbles are shown in Figs. 3(a) and 3(d), respectively. It can be seen that both compressive (negative) stress and tensile (positive) stress are generated. Specifically, the compressive stress appears as the surrounding tissue is compressed by the bubble, whereas the tensile stress is generated when the deformed tissue is restored to its original configuration. These temporal evolutions of the stress are consistent well with those of the mechanical stress generated by a single bubble as reported in previous studies by Mancia *et al.*[18,19] and Qin *et al.*[46]

To illustrate the spatial distribution of the stress, figures 3(b) and 3(e) display the compressive (τ_C) and tensile (τ_T) stresses surrounding the small and large bubbles as a function of the angle θ_1 ($\theta_1 = 0$–2π; $r_{1,b} = 3$ μm) and θ_2 ($\theta_2 = 0$–2π; $r_{2,b} = 3$ μm), respectively. The results indicate that both stresses surrounding the affected bubble with small initial radius (*i.e.*, the compressive stress $\tau_{C,w}$ and tensile stress $\tau_{T,w}$) first increase and then decrease as θ_1 increases, showing a larger variation in the compressive stress ($\tau_{C,w}$). This observation can be accounted for the superimposed effects of two stress fields generated by the small and large bubbles, as indicated in Eq. (11). By contrast, the stresses of the small bubble for the isolated case (*i.e.* the compressive stress $\tau_{C,w/o}$ and tensile stress $\tau_{T,w/o}$ shown in Fig. 3(b)) and those for the large

bubble for both two cases (*i.e.*, $\tau_{C,w}$, $\tau_{T,w}$, $\tau_{C,w/o}$, and $\tau_{T,w/o}$ shown in Fig. 3(e)) remain unchanged with the angel (*i.e.*, θ_1 for the small bubble and θ_2 for the large bubble) increasing. It can be explained that the stress field produced by the small bubble is much smaller than that by the large bubble (Figs. 3(a) and 3(d)), consequently leading to the negligible influence of the superimposed effects on the stress surrounding the large bubble. Moreover, the mechanical stresses are dramatically reduced by increasing the distance of the considered position from the bubble wall (*i.e.* $r_{1,b}$ for the small bubble and $r_{2,b}$ for the large bubble), especially for the tensile stress (Figs. 3(c) and 3(f)).

The comparison between the results with and without considering the effects of the adjacent bubble demonstrates that the effects of the large bubble can dramatically reduce the cavitation-associated stresses surrounding the small bubble. Conversely, the effects of the small bubble on the stresses surrounding the large bubble are negligible. This observation is in good agreement with the bubble dynamic behavior shown in Fig. 2, implying the high dependence of the cavitation-associated stress on bubble dynamics. More importantly, the superposition of two stress fields generated by each bubble results in nonuniform stress distribution surrounding the small bubble, exhibiting a much smaller stress in the same direction with the large bubble, *i.e.* $\theta_i = 0$ as defined in Fig. 1 ($i = 1$). These results highlight the necessity of taking the effects of the adjacent bubble into account while investigating the cavitation-mediated applications, in which multiple bubbles are generally formed and the mechanical stresses generated by these cavitation bubbles are related to the applications.

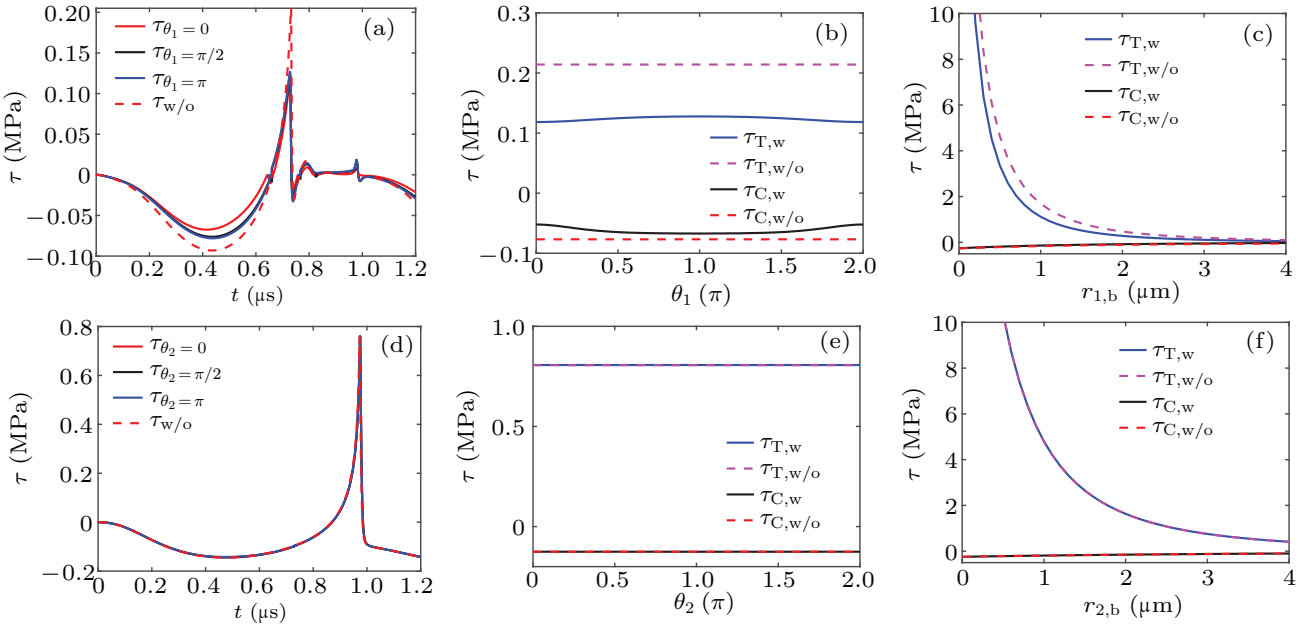


Fig. 3. Spatiotemporal evolutions of cavitation-associated stresses in tissue surrounding (a)–(c) small and (d)–(f) large bubbles for two cases with (w) and without (w/o) considering the effects of adjacent bubble. (a) Stress *versus* time at $r_{1,b} = 3$ μm, compressive and tensile stresses *versus* (b) θ_1 ($r_{1,b} = 3$ μm) and (c) $r_{1,b}$ ($\theta_1 = 0$). (d)–(f) Corresponding results for large bubble.

3.3. Influence of ultrasound amplitude

The influences of the ultrasound amplitude ($p_A = 0.1$–1 MPa) on the cavitation dynamics and the resultant mechanical stresses surrounding two-interacting and two isolated bubbles are shown in Fig. 4, indicating that the values of expansion ratio R' and maximum magnitude of stress τ', including the tensile (τ'_T) and compressive (τ'_C) stresses, of both bubbles increase as the ultrasound amplitude increases. Figure 4(a) shows that the expansion ratio of the small bubble (R'_1) is significantly reduced when considering the effects of the adjacent bubble (*i.e.* $R'_w < R'_{w/o}$). Moreover, the difference is amplified with the ultrasound amplitude increasing. Figures 4(b) and 4(c) display the maximum tensile stress and compressive stress of the small bubble, respectively. Considering the nonuniform stress distribution ascribed to the effects of the adjacent bubble, the maximum stresses in the three representative directions ($\theta_1 = 0$, $\pi/2$, and π; $r_{1,b} = 3$ μm) are compared with the counterparts in the case where the effects of the adjacent bubble are not considered. It can be seen that the effects of the adjacent bubble lead all the maximum stresses to decrease. Note that, the reduction increases with the ultrasound amplitude increasing, but decreases with the augment of θ_1, hence achieving the maximum reduction at $p_A = 1$ MPa and $\theta_1 = 0$. For the large bubble, similar variation tendency is presented in Figs. 4(d)–4(f), except that much smaller influences of the adjacent bubble are exerted on the expansion ratio and maximum stresses. These results further prove that the large bubble exerts a more significant influence on the neighboring small bubble and their mutual interactions are much stronger at higher acoustic pressures.

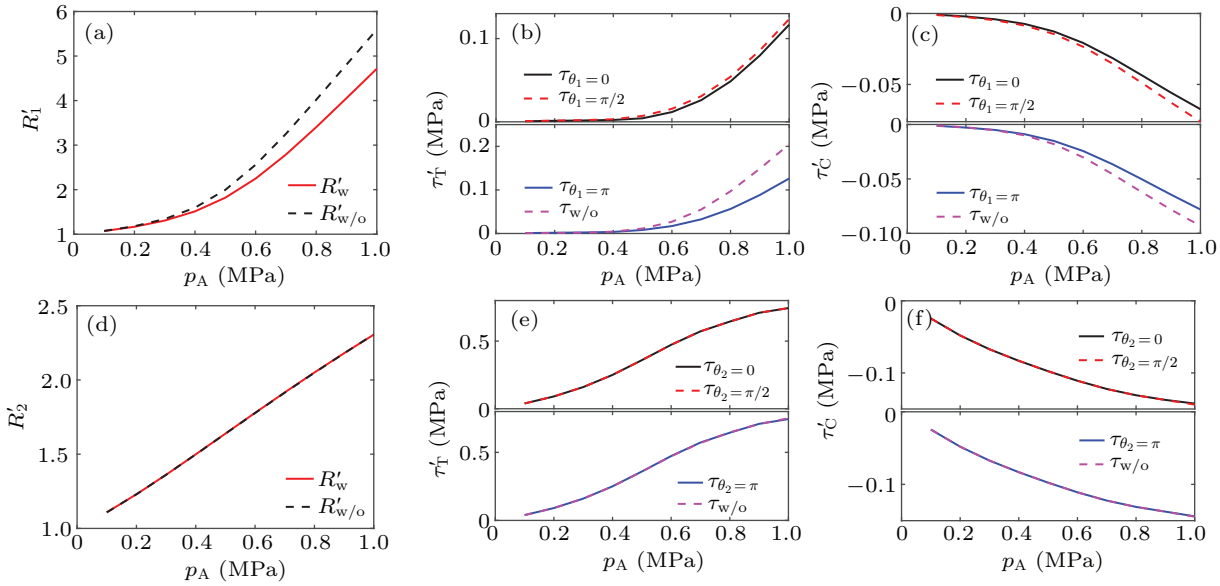


Fig. 4. Cavitation dynamics and associated mechanical stresses at different ultrasound amplitudes ($p_A = 0.1$ MPa–1 MPa). (a)–(c) Expansion ratio (R_1'), the maximum magnitude of tensile stress (τ_T'), and compressive (τ_C') stress *versus* p_A of the small bubble, while panels (d)–(f) are these of the large bubbles, respectively.

3.4. Quantifying effects of adjacent bubble on cavitation dynamics and stress

The effects of the adjacent bubble on the cavitation dynamics and its mechanical stress are further quantified by introducing two variables defined as absolute variation of the expansion ratio ($\Delta R'$) and the maximum stress magnitude ($\Delta\tau'$). For the i-th bubble, these variables can be expressed as

$$\Delta R_i' = \left|R_{i,\mathrm{w}}'\right| - \left|R_{i,\mathrm{w/o}}'\right|, \tag{13}$$

$$\Delta\tau_i' = \left|\tau_{i,\mathrm{w}}'\right| - \left|\tau_{i,\mathrm{w/o}}'\right|, \quad (i = 1,2), \tag{14}$$

where $R_{i,\mathrm{w}}'$, $R_{i,\mathrm{w/o}}'$, $\tau_{i,\mathrm{w}}'$, and $\tau_{i,\mathrm{w/o}}'$ denote the expansion ratios (R') and maximum stress magnitudes (τ') of the i-th bubble during the cavitation with (w) and without (w/o) considering the effects of the nearby bubble, respectively. The symbol $||$ denotes the absolute value of the variables. As indicated in Eqs. (13) and (14), the suppression effects of the adjacent bubble on the cavitation dynamics and the resultant stress can be described as $\Delta R' < $ and $\Delta\tau' < 0$ respectively, so can the case $\Delta R' > 0$ and $\Delta\tau' > 0$.

3.4.1. Influences of inter-bubble distance and initial radius of large bubble

Owing to the strong effects of large bubble on the small bubble, we mainly focus on the cavitation dynamics of the small bubble and the resultant mechanical stress in the surrounding tissues.

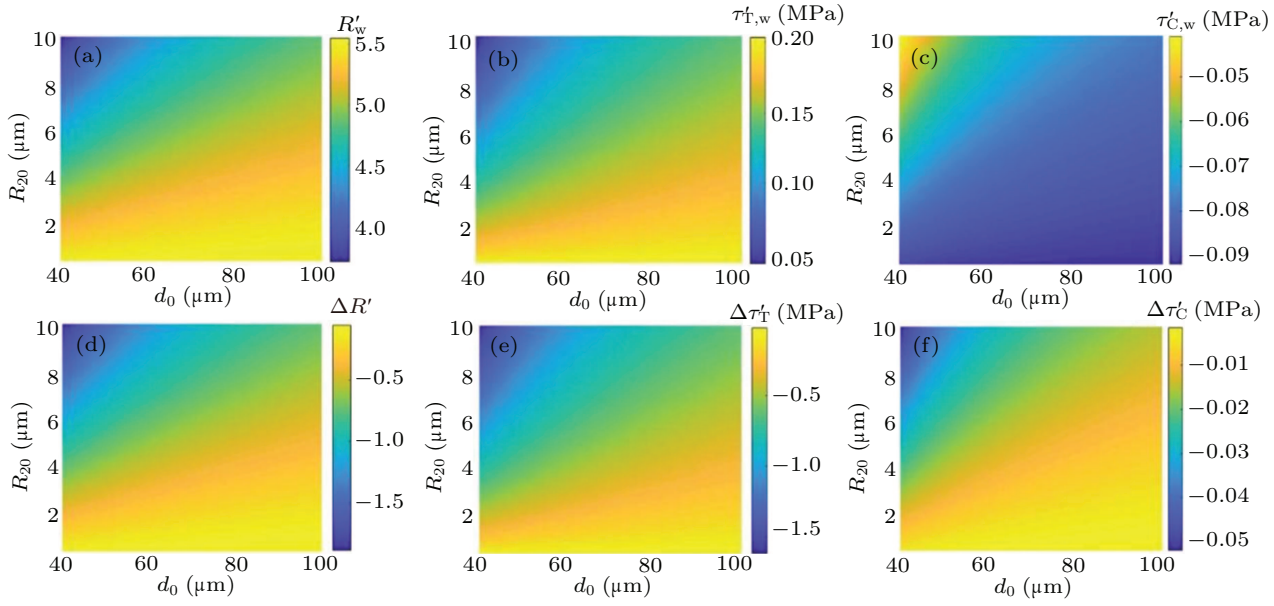


Fig. 5. Effects of inter-bubble distance ($d_0 = 40$ μm–100 μm) and the initial radius of large bubble ($R_{20} = 1$ μm–10 μm) on the cavitation dynamics of a 1-μm-radius bubble and the associated stress in the surrounding tissues. (a)–(c) Bubble expansion ratio (R_w'), maximum values of tensile stress ($\tau_{T,w}'$), and compressive stress ($\tau_{C,w}'$) , and (d)–(f) their absolute variation values ($\Delta R'$, $\Delta\tau_T'$, $\Delta\tau_C'$) compared with the case without considering the effects of adjacent bubble are displayed.

Figure 5 illustrates the influences of the inter-bubble distance (d_0 = 40 μm–100 μm) and the initial radius of the large bubble (R_{20} = 1 μm–10 μm) on the cavitation dynamics and the resultant mechanical stresses of a 1-μm-radius bubble. It is evident that for the bubble expansion ratio ($R'_{\rm w}$), maximum values of the compressive stress ($\tau'_{\rm C,w}$) and tensile ($\tau'_{\rm T,w}$) stress ($\theta_1 = 0$, $r_{1,\rm b} = 3$ μm) increase with d_0 increasing, but decrease as the R_{20} increases as illustrated in Figs. 5(a)–5(c), respectively. Furthermore, the absolute variations of $R'_{\rm w}$, $\tau'_{\rm C,w}$, and $\tau'_{\rm T,w}$ (defined as $\Delta R'$, $\Delta\tau'_{\rm C}$, and $\Delta\tau'_{\rm T}$) are displayed in Figs. 5(d)–5(f), respectively. The results demonstrate that these absolute variations are negative, suggesting that the effects of the adjacent bubble will suppress the small bubble expansion and lead the cavitation-associated stresses to decrease. In addition, it is obvious that the suppression effects can be enhanced by reducing the inter-bubble distance and/or increasing the initial radius of the large bubble, which is consistent with previous results.[22,34] Compared with the inter-bubble distance, the initial radius of the adjacent bubble seems to have a strong influence on the suppression effects. From another point of view, these results also suggest that the influence of mutual interactions of multiple bubbles on the bubble dynamics and its mechanical stress can be predicted according to the concentration and size distribution of the bubbles.

3.4.2. Influence of tissue viscoelasticity

Figure 6 exemplifies the influences of the tissue viscoelasticity (G = 0 kPa–500 kPa, μ = 1 mPa·s–50 mPa·s) on the cavitation dynamics and the resultant mechanical stresses of the small bubble at $\theta_1 = 0$, $r_{1,\rm b} = 3$ μm. The expansion ratio of the small bubble and its associated mechanical stress varying with the tissue elasticity and viscosity are displayed in Figs. 6(a), 6(b), 6(d), and 6(e), respectively. The results demonstrate that the bubble oscillations and its mechanical stresses decrease with the tissue viscoelasticity increasing, except that the tensile stress and compressive stress first increase and then decrease as the tissue viscosity and elasticity increase respectively. Similar changes are observed in the suppression effects of the neighboring bubble on the cavitation dynamics and mechanical stress (*i.e.* $\Delta R'$, $\Delta\tau'_{\rm T}$, and $\Delta\tau'_{\rm C}$ shown in Figs. 6(c) and 6(f)). These discrepancies may be explained by the fact that both compressive and tensile stresses are determined not only by the bubble dynamics which is affected by the tissue viscoelasticity, but also directly by the tissue elasticity and viscosity as indicated in Eq. (5). Moreover, it may also suggest that the direct influence of the tissue viscoelasticity on the stress seems to be the primary factor within the parameters examined in this paper.

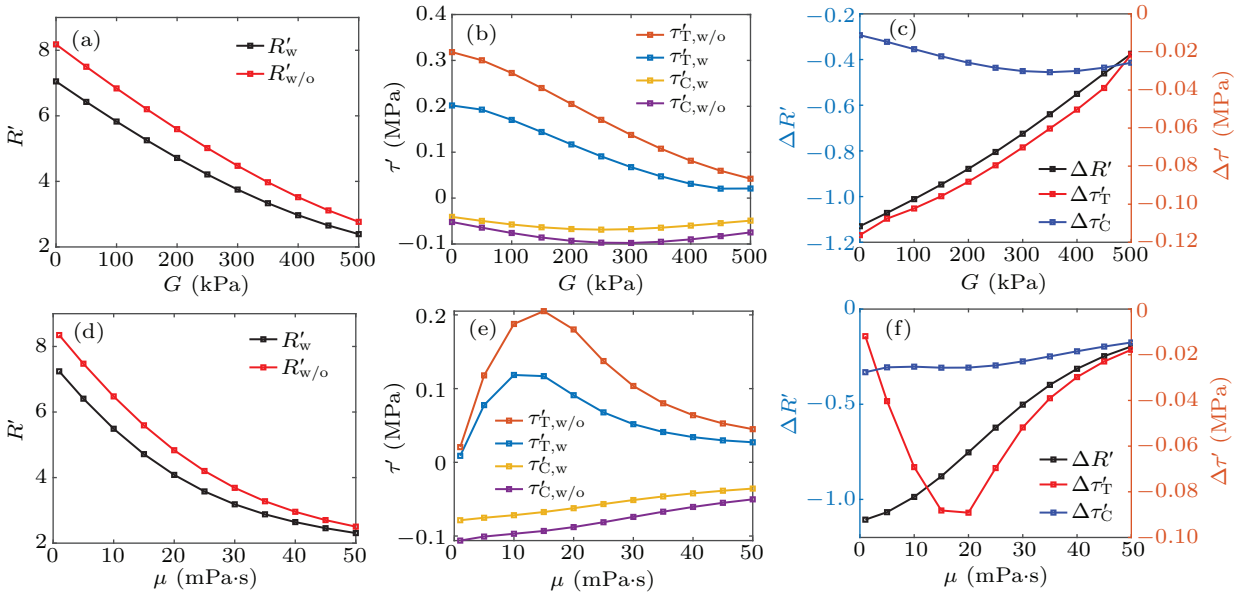


Fig. 6. Effects of tissue viscoelasticity on cavitation dynamics and associated stress in the surrounding tissues for two cases with and without considering effects of the neighboring bubble (G = 0 kPa–500 kPa, μ = 1 mPa·s–50 mPa·s). (a) Expansion ratio (R'), (b) tensile stress ($\tau'_{\rm T}$) and compressive ($\tau'_{\rm C}$) stress, (c) their absolute variation values of expansion ratio and stresses *versus* tissue elasticity, and (d)–(f) corresponding results as a function of tissue viscosity.

4. Conclusions

The cavitation dynamics of two-interacting bubbles and the associated mechanical stresses in the surrounding tissue are numerically investigated in this study. The spatiotemporal evolutions of the stress indicate that the cavitation-associated stress is highly dependent on the time-varying bubble dynamics, *i.e.*, compressive stress and tensile stress are generated during the explosive bubble expansion and violent bubble collapse respectively. Moreover, larger stresses are observed near the bubble wall, and nonuniform stress distributions surrounding the bubbles are caused by the superposition of two stress fields generated by each bubble, resulting in a much

smaller stress in the direction of the adjacent bubble. Compared with the cases of the isolated bubbles, the effects of the adjacent bubble can notably restrain the cavitation dynamics of the small bubble and consequently reduce the cavitation-associated stresses. Targeting the case of significantly affected bubble with small initial radius, the suppression effects of the neighboring bubble can be intensified by increasing the ultrasound amplitude and initial radius of the large bubble, or reducing the inter-bubble distance and tissue viscoelasticity. This study can provide a further insight into the effects of adjacent bubbles on the cavitation dynamics and associated stress in viscoelastic tissue.

Acknowledgements

Project supported by the National Natural Science Foundation of China (Grant No. 11904042), the Natural Science Foundation of Chongqing, China (Grant No. cstc2019jcyj-msxmX0534), and the Science and Technology Research Program of Chongqing Municipal Education Commission, China (Grant No. KJQN202000617).

References

[1] Brennen C E 2014 *Cavitation and bubble dynamics* (Cambridge: Cambridge University Press) pp. 196–197
[2] Wan M, Feng Y and ter Haar G 2015 *Cavitation in biomedicine* (Springer) pp. 1–5
[3] Yusof N S M, Babgi B, Alghamdi Y, Aksu M, Madhavan J and Ashokkumar M 2016 *Ultrason. Sonochem.* **29** 568
[4] Bhargava N, Mor R S, Kumar K and Sharanagat V S 2021 *Ultrason. Sonochem.* **70** 105293
[5] Al Sawaftah N M and Husseini G A 2020 *J. Nanosci. Nanotechnol.* **20** 7211
[6] Teng X D, Guo X S, Tu J and Zhang D 2016 *Chin. Phys. B* **25** 124308
[7] Stride E and Coussios C 2019 *Nat. Rev. Phys.* **1** 495
[8] Zhang D Y, Wan Y, Xu J Y, Wu G H, Li L and Yao X H 2016 *Carbohydr. Polym.* **137** 473
[9] Ahmadi A, Hosseini Nami S, Abed Z, Beik J, Aranda Lara L, Samadian H, Morales-Avila E, Jaymand M and Shakeri Zadeh A 2020 *Drug Discov. Today* **12** 2182
[10] Yu J, Chen Z and Yan F 2019 *Prog. Biophys. Mol. Biol.* **142** 1
[11] Novell A, Kamimura H, Cafarelli A, Gerstenmayer M, Flament J, Valette J, Agou P, Conti A, Selingue E and Badin R A 2020 *Sci. Rep.* **10** 1
[12] Suo D, Jin Z, Jiang X, Dayton P A and Jing Y 2017 *Appl. Phys. Lett.* **110** 023703
[13] Zhang L, Wang X D, Liu X Z and Gong X F 2015 *Chin. Phys. B* **24** 014301
[14] Maxwell A D, Cain C A, Duryea A P, Yuan L, Gurm H S and Xu Z 2009 *Ultrasound Med. Biol.* **35** 1982
[15] Yuan F, Yang C and Zhong P 2015 *Proc. Nat. Acad. Sci.* **112** E7039
[16] Vlaisavljevich E, Maxwell A, Mancia L, Johnsen E, Cain C and Xu Z 2016 *Ultrasound Med. Biol.* **42** 2466
[17] Qin D, Zhang L, Chang N, Ni P, Zong Y, Bouakaz A, Wan M and Feng Y 2018 *Ultrason. Sonochem.* **47** 141
[18] Mancia L, Vlaisavljevich E, Xu Z and Johnsen E 2017 *Ultrasound Med. Biol.* **43** 1421
[19] Mancia L, Vlaisavljevich E, Yousefi N, Rodriguez M, Ziemlewicz T J, Lee F T, Henann D, Franck C, Xu Z and Johnsen E 2019 *Phys. Med. Biol.* **64** 225001
[20] Edsall C, Khan Z M, Mancia L, Hall S, Mustafa W, Johnsen E, Klibanov A L, Durmaz Y Y and Vlaisavljevich E 2021 *Ultrasound Med. Biol.* **47** 620
[21] Zilonova E, Solovchuk M and Sheu T 2018 *Ultrason. Sonochem.* **40** 900
[22] Zilonova E, Solovchuk M and Sheu T 2019 *Phys. Rev. E* **99** 023109
[23] Zilonova E, Solovchuk M and Sheu T 2019 *Ultrason. Sonochem.* **53** 11
[24] Rezaee N, Sadighi Bonabi R, Mirheydari M and Ebrahimi H 2011 *Chin. Phys. B* **20** 087804
[25] Wang D and Naranmandula 2018 *Acta Phys. Sin.* **67** 037802 (in Chinese)
[26] Zhang Y L, Zheng H R, Tang M X and Zhang D 2011 *Chin. Phys. B* **20** 114302
[27] Liang J F, Wu X Y, Yu A, Chen W Z and Wang J 2020 *Chin. Phys. B* **29** 097801
[28] Zhang L L, Chen W Z, Shen Y, Wu Y R, Zhao G J and Kou S Y 2022 *Chin. Phys. B* **31** 044303
[29] Qinghim and Naranmandula 2019 *Acta Phys. Sin.* **68** 234302 (in Chinese)
[30] Mo R Y, Wang C H, Hu J and Chen S 2019 *Acta Phys. Sin.* **68** 144302 (in Chinese)
[31] Li X, Chen Y, Feng H and Qi L 2020 *Acta Phys. Sin.* **69** 184703 (in Chinese)
[32] Zhang L L, Chen W Z, Zhang Y Y, Wu Y R, Wang X and Zhao G Y 2020 *Chin. Phys. B* **29** 034303
[33] Chen H, Lai Z, Chen Z and Li Y 2019 *Ultrason. Sonochem.* **52** 344
[34] Qin D, Zou Q, Lei S, Wang W and Li Z 2021 *Ultrason. Sonochem.* **78** 105712
[35] Zhang L L, Chen W Z, Wu Y R, Shen Y and Zhao G Y 2021 *Chin. Phys. B* **30** 104301
[36] Shen Y, Zhang L, Wu Y and Chen W 2021 *Ultrason. Sonochem.* **73** 105535
[37] Wang C H and Cheng J C 2013 *Chin. Phys. B* **22** 014304
[38] Estrada J B, Barajas C, Henann D L, Johnsen E and Franck C 2018 *J. Mech. Phys. Solids* **112** 291
[39] Estrada J B, Luetkemeyer C M, Scheven U M and Arruda E M 2020 *Exp. Mech.* **60** 907
[40] Gaudron R, Murakami K and Johnsen E 2020 *J. Mech. Phys. Solids* **143** 104047
[41] Gaudron R, Warnez M and Johnsen E 2015 *J. Fluid Mech.* **766** 54
[42] Kanthale P M, Brotchie A, Ashokkumar M and Grieser F 2008 *Ultrason. Sonochem.* **15** 629
[43] Hegedüs F, Klapcsik K, Lauterborn W, Parlitz U and Mettin R 2020 *Ultrason. Sonochem.* **67** 105067
[44] Kalmár C, Klapcsik K and Hegedüs F 2020 *Ultrason. Sonochem.* **64** 104989
[45] Kanthale P M, Gogate P R and Pandit A B 2007 *Chem. Eng. J.* **127** 71
[46] Qin D, Zou Q, Li Z, Wang W, Wan M and Feng Y 2021 *Acta Phys. Sin.* **70** 148 (in Chinese)